JOURNAL OF SOLID STATE CHEMISTRY 24, 265–275 (1978)

Ionic Conductivity of Pure and Doped Na_3PO_4

A. HOOPER,* P. McGEEHIN,* K. T. HARRISON,* AND B. C. TOFIELD†

Materials Development Division and †Materials Physics Division, Harwell, Oxfordshire, England

Received June 6, 1977; in revised form September 15, 1977

The ionic conductivity of pure and doped polycrystalline trisodium orthophosphate (Na_3PO_4) has been measured, using an ac technique, from 150 to 350°C. For the pure material, $\sigma(300°C) \sim 5 \times 10^{-3}\ \Omega^{-1}\ cm^{-1}$. Enhancement of conductivity is not achieved by doping with $AlPO_4$, Na_2SO_4, or Na_4SiO_4 and activation energies in all cases are in the range 0.8–1.0 eV. At high levels of doping a low-melting-point glass, with good ionic conductivity, is produced in the Na_3PO_4–$AlPO_4$ system. Conductivity values are also reported for a sample of polycrystalline Ag_3PO_4.

1. Introduction

Recent development of the sodium–sulfur battery and similar systems (*1*) has stimulated and maintained interest in fast ion conducting solid electrolytes (*2*). In the battery, polycrystalline sodium β-alumina acts as the separator between the electrodes, and its high sodium ion conductivity at around 300°C enables appreciable current to be drawn from the cell. There is a need both for a fundamental understanding of the properties of fast ion conductors like β-alumina, and for the discovery and characterization of new materials which may have improved properties. In this paper we present results on high sodium concentration compounds based on trisodium orthophosphate, Na_3PO_4. The electrical properties of the materials investigated have been studied using complex plane plotting to interpret ac conductivity data (*3*).

The crystal structure of Na_3PO_4 is apparently not known. However, Palazzi and Remy (*4*) observed a transition at around 300°C from a tetragonal to a face-centered cubic cell and quoted for the high-temperature phase, γ-Na_3PO_4, a lattice constant of 7.413(2) Å at 25°C.[1] Examination of possible space groups for the high-temperature phase shows the possibility of sodium disorder; an indicator of possible fast sodium ion conductivity. A possible analogy is found with lithium sulfate, which also has a face-centered cubic cell, a = 7.07 Å (*5*), at high temperature.

The face-centered cubic α phase of Li_2SO_4, which is stable between 575°C and the melting point at 870°C, has one of the highest known lithium ion conductivities of $\sim 1\ \Omega^{-1}\ cm^{-1}$, albeit at the elevated temperature of ~600°C, and an activation energy around 0.36 eV (*6*). On melting the conductivity increases by only 28% (*6*). The low-temperature monoclinic β phase has a much reduced conductivity with an activation energy greater than 2 eV (*6*). As the cubic γ-Na_3PO_4 phase is reported (*4*) to be stabilized at room temperature by the addition of $AlPO_4$, we were encouraged to investigate the possibility that high alkali ion conductivity might be observed at temperatures lower than the phase transition of the pure material, as is found in α-

[1] It would appear that a small degree of aluminum doping was necessary to retain the γ-phase on cooling to room temperature.

0022-4596/78/2434-0265$02.00/0

Li_2SO_4 when doped with a variety of other materials. Since, in both the sulfates and β-aluminas, silver mobility is often associated with that of sodium, we have also investigated the ionic conductivity of Ag_3PO_4, although the conductivity extrapolated from the work of Takahashi *et al.* (*7*) on AgI–Ag_3PO_4 did not give rise to optimism.

γ-Na_3PO_4 is also of interest in that the sodium ion concentration is considerably higher than that of sodium β-alumina, the high decomposition point (~1450°C) makes it more amenable to ceramic processing than the waxy lithium sulfates, and the cubic symmetry reduces problems of anisotropic thermal expansion found with β-alumina in device applications. It also offers the chance to study sodium ion conductivity in a compound containing discrete anions rather than an infinite anionic framework as in β-alumina and $Na_3Zr_2PSi_2O_{12}$ (*8*). Lithium conductivity has been studied recently, for example, in the related orthogermanates and orthosilicates (*9–11*), but Na_2WO_4 is the only simple anionic sodium compound showing fast ionic conductivity on which data have been reported (*12*). Like Li_2SO_4, this compound shows a greater than two orders of magnitude increase in conductivity on heating through the $\gamma \rightarrow \beta$ phase transformation at the relatively high temperature of ~590°C. We should of course note that although we have invoked above an analogy between the lattice constants of γ-Na_3PO_4 and α-Li_2SO_4 in order to justify study of the former, a comparison, for example, of Na and Li β-alumina (*13*) indicates that many aspects of sodium and lithium ion motion may be considerably different from one another.

We have studied both pure[2] Na_3PO_4 and Ag_3PO_4, and also Na_3PO_4 doped with Na_4SiO_4, Na_2SO_4 and, particularly, $AlPO_4$. The first dopant induces a cation excess, while the latter two produce vacancies. Using both these approaches, it was hoped to modify rapid ion diffusion in much the same way as Kvist *et al.* (*14*) have done by doping *fcc* Li_2SO_4 with LiCl and $MgSO_4$.

[2] Actually, our preparative route from "$Na_3PO_4 \cdot 12H_2O$" entails a small NaOH impurity level. We do not believe this affects the conclusions to any significant extent.

2. Experimental

2.1. Specimen Preparation

Conductivity specimens were made using technical grade $Na_3PO_4 \cdot 12H_2O$ dried in vacuum at ~160°C overnight to remove water of crystallization. Doped samples were prepared by the addition of either dried technical grade $AlPO_4$, "Analar" Na_2SO_4, or a mixture of general purpose precipitated silica and "Analar" Na_2CO_3. All powder mixtures were blended in a ball-mill (alumina balls) under acetone (aluminum and silicate doped) or petroleum ether (sulfate doped) overnight (aluminum doped) or for ~4 h (silicate and sulfate doped). The resultant slurry was gently heated to evaporate the solvent and the cake mechanically crushed. Following calcination at or slightly below the final sintering temperature, the powder was again mechanically crushed and sieved to <53 μm (silicate and sulfate) or <106 μm (aluminum doped). Pellets ~1 cm in diameter and a few millimeters thick were produced by compaction in a conventional steel die at a pressure of ~150 MPa and fired at the temperatures given in Table I. These temperatures were chosen to be ~30°C (low-temperature firings) or as much as 100°C (high-firing temperatures) below the melting points of the respective mixtures. In doubtful cases this temperature was determined using a Linseis L81 DTA apparatus, which was also used to study the temperatures at which phase changes occurred in the finished conductivity specimens. The course of the solid-state reactions was followed and checked using a Phillips Debye–Scherrer X-ray powder camera. Fired pellets were cleaned and their density measured pycnometrically using acetone, prior to the flats being polished with 6-μm diamond paste and evaporated gold contacts (~1 μm thick) being applied.

TABLE I

EXPERIMENTAL DETAILS OF CONDUCTIVITY SPECIMENS

	Final sintering temperature (°C)	Lattice parameter if cubic (Å) (error 0.01 Å)	Density (% of theoretical)
$Na_{3(1-x)}Al_xPO_4$			
$x = 0$	1350	Tetragonal	89.3[a]
$x = 0.01$	1350	Tetragonal	90.4[a]
$x = 0.025$	1350	Tetragonal	96.3[a]
$x = 0.05$	1350	7.45 (quenched)	91.3[a]
$x = 0.1$	1350	7.45 (Slow cooled and quenched)	93.8
$x = 0.2$	1150	7.41	95.3
$x = 0.3$	1100	7.42	97.2
$x = 0.4$	875	7.41	98.8
$x = 0.6$	Glass at ~460°C		
$Na_{3(1+x)}P_{1-3x}Si_{3x}O_4$			
$x = 0.033$	1000	7.48	91.8
$x = 0.066$	1000	7.48	94.3
$x = 0.166$	850		
$Na_{3(1-x)}P_{1-3x}S_{3x}O_4$			
$x = 0.05$	700	7.46	81.6
$x = 0.1$	700	7.46	74.6
$x = 0.2$	700		
Ag_3PO_4	850	[b] Room temp 6.0095(6) at 650°C, 7.737(1)	90.8

[a] Density estimated using lattice parameters of pure Na_3PO_4 (low-temperature phase).

[b] From X-ray single crystal (room temperature) and powder neutron (high temperature) diffraction data (*15*).

2.2. *Conductivity Measurements*

Electrical contact was made via platinum foils in pressure contact with the evaporated electrodes, and ac conductivity measurements were made in air with silica gel as a drying agent over the temperature range 150–350°C. The apparatus consisted of a Solartron frequency response analyser 1172 in conjunction with a standard series resistance (1–10 kHz) and Wayne Kerr bridges B 221/B 601 with external source (Krohn–Hite 4200) and detector (Marconi TF 1100) (500 Hz–1 MHz). Consistent results were obtained with both types of equipment in the region of overlapping frequency. Reproducibility was also observed on remeasuring selected samples at later times.

The measured conductivities quoted in Section 3 were all taken at a frequency of 10 kHz, but prior to the adoption of this fixed frequency technique the complete response from 1 Hz to 1 MHz of selected specimens at a variety of temperatures was assessed by the use of complex plane analysis. The observed form of the complex admittance plot (G vs B) changes in a progressive manner with temperature (Fig. 1). At low temperatures a typical plot corresponds essentially to a parallel R and C combination, where C represents the geometrical capacitance of the specimen and R its resistance. At high temperatures an interfacial capacitance, caused by the pileup of mobile ions at the blocking electrodes, dominates the electrical response; the appropriate equivalent

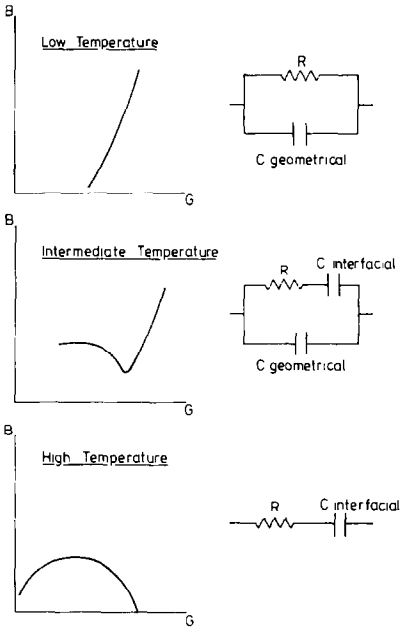

FIG. 1. A schematic representation of the observed complex admittance behavior, with appropriate equivalent circuits, of sodium phosphate (pure and doped) samples. The absolute values of temperature within each regime vary with specimen composition.

circuit is then a series R, C combination with R still the specimen resistance. At intermediate temperatures the two types of plot merge together, the point at which one dominates over the other being determined by the relative values of the equivalent circuit components. The higher the specimen conductivity, the lower the transition temperature to the series form. In all cases, however, the value of R is found at the point corresponding to the minimum value of B. This point, of course, occurs at a different frequency for different specimens and temperature, but in this instance it was apparent that, at least for the higher conductivity samples in the temperature regime of most interest (200–300°C), 10-kHz values would lead to negligible error in R. Any errors which do occur at this upper end of the temperature range for the high conductivity samples will lead to pessimistic conductivity values. We should note that it is impossible to decide absolutely on the real significance of the circuit component R. Accordingly, for the purposes of this paper, it is regarded as an overall electrolyte resistance including, in particular, both intra- and intergrain contributions. In reality, for example, grain boundaries will be represented by a combination of resistive and capacitative terms, but these have not been resolved. Deviations in the complex plane plots from the ideal equivalent circuit behavior probably arise from interfacial effects. They do not affect the derived values of electrolyte resistance which are the primary target of this work.

3. Experimental Results

3.1. Crystallography

Stability of the cubic γ-Na_3PO_4 phase was achieved at room temperature, as described by Palazzi and Remy (*4*), by doping with $AlPO_4$ to produce compositions of nominal concentration $Na_{3(1-x)}Al_x\square_{2x}PO_4$, where $\square$ represents a cation vacancy. In $Na_{3(1-x)}Al_xPO_4$ the cubic phase is obtained for $x \geqslant 0.1$; a few very faint background lines are also observed indicating a few percent of a second phase. The lattice parameter decreases (Table I) as the substitution of smaller Al^{3+} ions for Na^+ ions proceeds and the concentration of vacancies increases. When $x = 0.05$, the tetragonal phase is obtained on slow cooling; but air quenching gives predominantly the cubic phase with some tetragonal phase also present. Below $x = 0.05$ the tetragonal phase is observed almost exclusively, although careful examination of the X-ray powder patterns of both slow-cooled and quenched samples does indicate the presence of a small amount of the cubic phase. The α–γ phase transformation temperature of the tetragonal samples was investigated using DTA. For the pure compound, a value of 300°C (*4*) was confirmed and a figure of ~300°C also found for $x = 0.025$. In the case of $x = 0.05$ the phase change occurs at ~290°C, but only for the slow cooled "tetragonal" sample on heating for the first time. In the case of the $x = 0.1$ sample, which

is cubic at room temperature, no phase change was observed by DTA up to 430°C.

At $x = 0.6$, when the concentration of sodium ions equals that of the induced vacancies, a clear glass (giving only a diffuse peak on an X-ray powder diffraction photograph) is formed at a relatively low temperature ($T < 500$°C). Glasses of poorer quality were also formed for compositions $x = 0.4$ and $x = 0.5$ at ~900°C and ~605°C, respectively. A crystalline specimen of the former was made by sintering below 900°C, but this could not be achieved below 600°C for the latter. Glass formation has not to our knowledge been observed previously in this region of the Na_2O–Al_2O_3–P_2O_5 system.

For Na_3PO_4 doped with sulfate and silicate, the two lower dopings ($x = 0.05$, 0.1 and $x = 0.033$, 0.066, respectively; Table I) both gave X-ray powder patterns which could be indexed as face-centered cubic; $a = 7.46$ and 7.48 Å, respectively with only very few very faint extra lines visible. The highest doped silicate ($x = 0.166$) and sulfate ($x = 0.2$) both gave complicated diffraction patterns. Some of the lines could be indexed *fcc* as above, but there remained a number of unidentified lines which indicated the presence of additional phases. Attempts to fit these lines to the known patterns of the pure reagents failed.

Since this work has been primarily concerned with establishing compositions which show fast sodium ion conductivity, no attempt has been made to establish rigorous phase diagrams. Nevertheless, our results indicate a considerable degree of solubility for $AlPO_4$ in

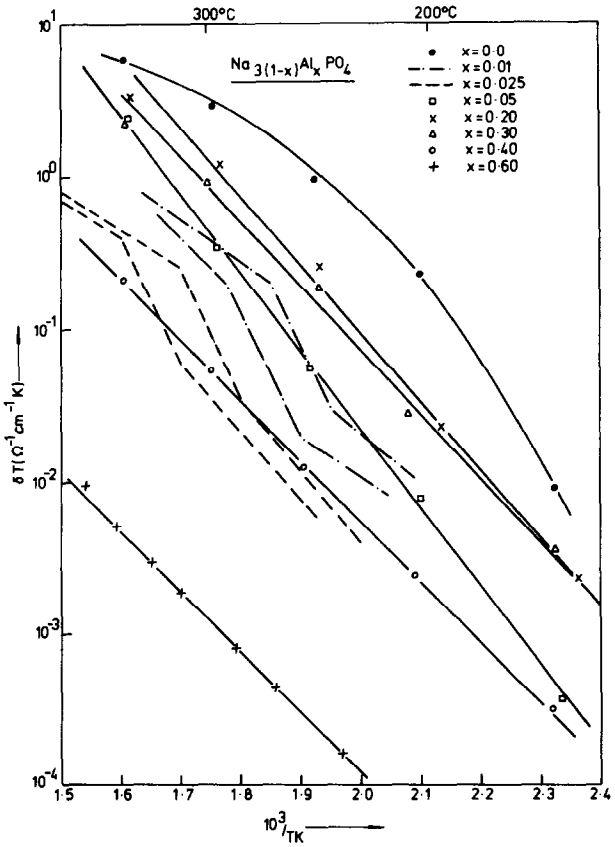

FIG. 2. Temperature dependence of the ionic conductivity of aluminum phosphate-doped sodium phosphate; $Na_{3(1-x)}Al_xPO_4$, $0.6 \geqslant x \geqslant 0$.

Na_3PO_4 with the high-temperature cubic phase[3] being stabilized at room temperature as reported previously (*4*). For the higher dopant levels, where the cubic phase is observed ($x \geqslant 0.2$), admixtures with the glassy phase are possible and would not have been established by analysis of X-ray powder diffraction patterns.

At room temperature Ag_3PO_4 has a primitive cubic cell (space group $P\bar{4}3n$) containing two formula units, but the structure determination was complicated by the presence of several anomalous reflections, which were interpreted as evidence of asymmetry in the thermal motion of the silver ions (*16*). On heating Ag_3PO_4 to 600°C, we observed silver particles and dendrites to appear on the surface of a compact. DTA showed a phase change at 553°C, and high-temperature neutron diffraction (*15*) has revealed that above the transition temperature Ag_3PO_4 also adopts a face-centered cubic cell. Refinement of the various structures of Ag_3PO_4 and Na_3PO_4 is in progress.

[3] High-temperature neutron diffraction (*15*) has confirmed the existence of the face-centered cubic phase in pure Na_3PO_4.

3.2. *Conductivity*

Figure 2 shows Arrhenius plots for the series of $AlPO_4$-doped samples. Over the measured temperature range (150–350°C) none of the doped materials has a conductivity higher than that of pure Na_3PO_4. For values of x (Table I) greater than and

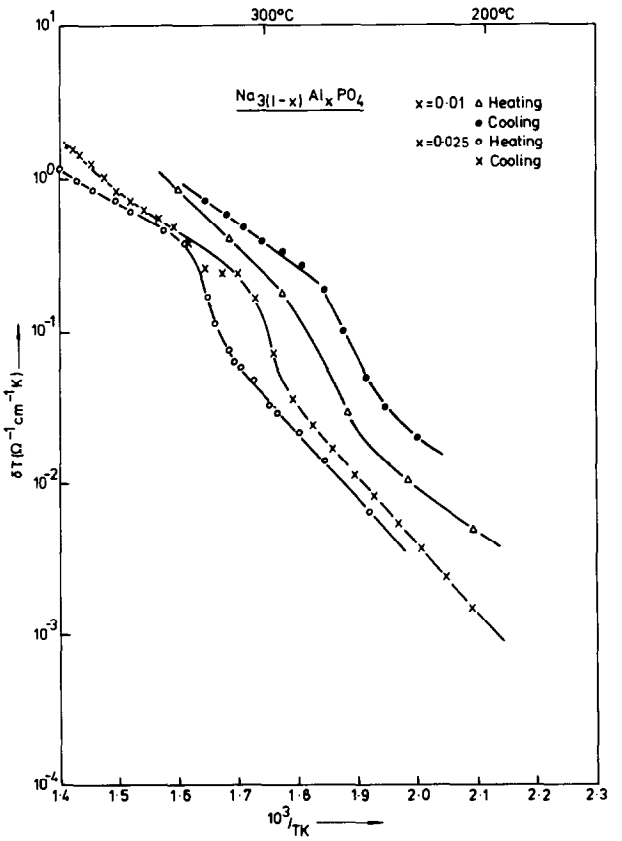

FIG. 3. Detailed temperature dependence of the ionic conductivity of $Na_{3(1-x)}Al_xPO_4$ for $x = 0.01$ and $x = 0.025$ showing a discontinuous rise around 300°C with some hysteresis.

including 0.05, the plots are reasonably straight lines with corresponding activation energies between 0.8 and 1.0 eV. The lower-doped compositions ($x = 0.01$, 0.025) exhibited a discontinuity in conductivity at around 300°C with some temperature hysteresis (Fig. 3). No such effects were observed for the pure material, although in this case the plot is curved. No hysteresis effects were observed either for the more highly doped compositions where the phase transition is not observed and the cubic phase is retained over the whole temperature region. This indicates that problems with water absorption are not a complicating factor in the interpretation. A graph of conductivity at 300°C (σ_{300}) versus composition (x) is shown in Fig. 6. A sharp decrease in conductivity is observed from pure material to a doping level of $x = 0.025$ followed by an increase maximizing at $x = 0.2$ and then by a smooth falling away for compositions with $x > 0.2$. The results for the glass composition of $x = 0.6$ indicate an activation energy of 0.8 eV and $\sigma_{300} \approx 2.10^{-6}$ Ω^{-1} cm^{-1}.

As shown in Fig. 4, doping with sodium sulfate again has the effect of decreasing the conductivity below that for pure Na_3PO_4. The decrease is fairly small for low doping levels, becoming large for $x > 0.1$. A plot of σ_{300} versus x is included in Fig. 6. The effect of doping with sodium silicate is illustrated in Fig. 5 and indicates once more a fall in conductivity with doping level. In this case, small doping levels lead to a sharp fall in conductivity followed by a tailing off at higher

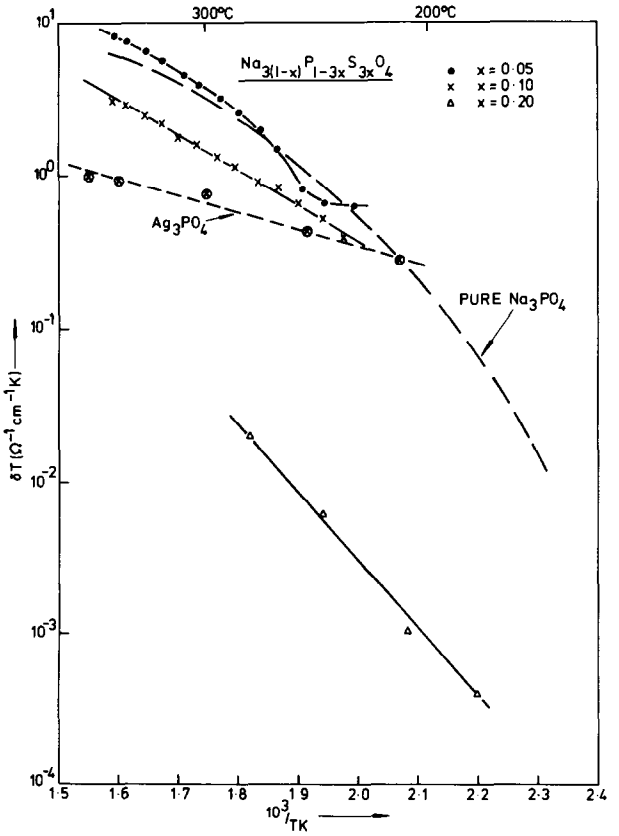

FIG. 4. Temperature dependence of the ionic conductivity of sodium sulfate-doped sodium phosphate; $Na_{3(1-x)}P_{1-3x}S_{3x}O_4$, $x = 0.05$, 0.1, 0.2, and of pure Ag_3PO_4.

concentrations (Fig. 6). Average activation energies are in the region of 0.8 eV.

Direct current (dc) measurements with gold electrodes have enabled the electronic contribution to the overall conductivity of these samples to be estimated. At 300°C, this electronic conductivity is typically 6 or 7 orders of magnitude below the ionic value.

Figure 4 contains a plot of log $\sigma T v 10^3/T$ for Ag_3PO_4, which has a lower value of σ_{300} than Na_3PO_4 but also a lower activation energy (0.45 eV), leading to an enhanced conductivity at temperatures below ~200°C.

4. Discussion

This work has shown that trisodium orthophosphate, Na_3PO_4, is a fast sodium-ion conductor at moderate temperatures (150–350°C). It is the first simple sodium salt with isolated anion groups so far reported to show such behavior in this temperature range. Doping with Al^{3+}, SO_4^{2-}, or SiO_4^{4-} ions does not enhance the conductivity, which for pure Na_3PO_4 at 300°C is $\sim 5.10^{-3}$ Ω^{-1} cm^{-1} compared with $\sim 10^{-1}$ Ω^{-1} cm^{-1} for polycrystalline sodium β-alumina. This conductivity and the fairly high activation energies (~0.8 eV) found for both pure and doped samples do not make these compounds realistic candidates for low-temperature (<300°C) battery systems. On heavy doping with $AlPO_4$, a hitherto unknown glass-forming composition was discovered with a minimum melting temperature at the composition $Na_{1.2}Al_{0.6}\square_{1.2}PO_4$. The sodium conductivity of

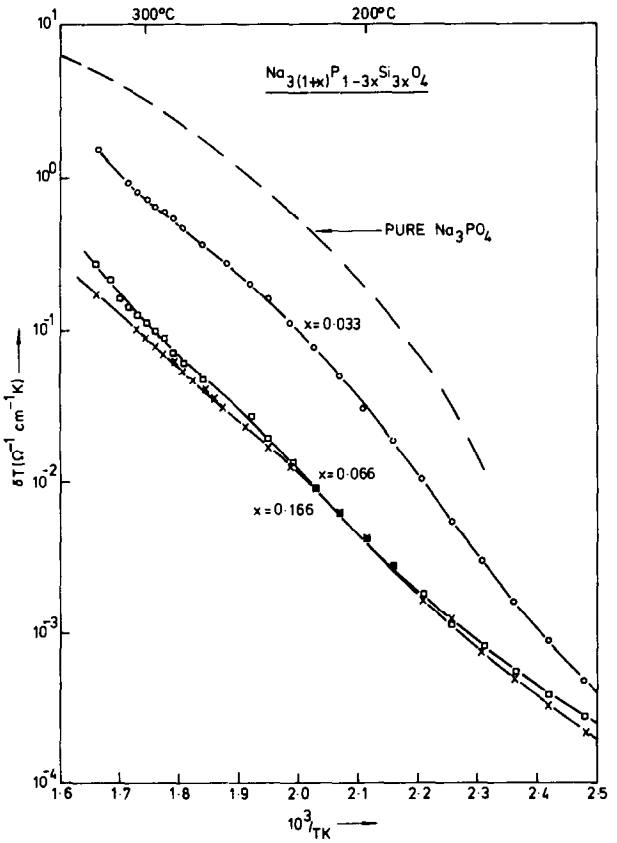

FIG. 5. Temperature dependence of the ionic conductivity of sodium silicate-doped sodium phosphate; $Na_{3(1+x)}P_{1-3x}Si_{3x}O_4$, $x = 0.033, 0.066, 0.166$.

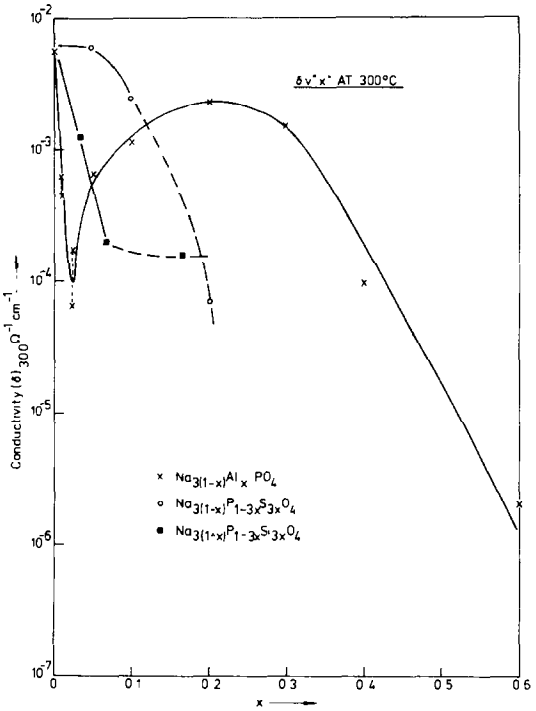

FIG. 6. Ionic conductivity as a function of composition (x) for aluminum phosphate-doped ($Na_{3(1-x)}Al_xPO_4$), sodium sulfate-doped ($Na_{3(1-x)}P_{1-3x}S_{3x}O_4$) and sodium silicate-doped ($Na_{3(1+x)}P_{1-3x}Si_{3x}O_4$) sodium phosphate.

this material is one of the highest observed for noncrystalline hosts. At 300°C, $\sigma \sim 2 \times 10^{-6}$ Ω^{-1} cm^{-1}, which is very similar to the optimum conductivities found in alkali borate glasses (*17*). A brief discussion of possible interpretations of the results is given followed by a comparison of the properties of simple lithium and sodium salts showing fast ion conductivity.

In the absence of detailed phase diagram and structural information on the systems studied, it is not possible to establish a viable microscopic rationale for the observed behavior. The situation is complicated by the fact that, because the dopants are not isovalent with the ions for which they substitute, there will be local attractive and repulsive coulombic terms that alter the potential distribution in the average cell. Any discussion of these effects requires detailed knowledge of both long- and short-range orders in the crystals, which is not presently available. Moreover, if significant amounts of second phases are present, considerable modifications of the macroscopic resistivity can be expected as discussed by Bauerle (*3*) for the case of zirconia–yttria solid solutions. Such effects may be expected to be most apparent at higher dopant levels.

Figure 2 shows that for pure Na_3PO_4, the first-order transition observed by DTA is not manifested by a discontinuity by the ionic conductivity. This is surprising, but may reflect a very sluggish phase change or a partially disordered sodium lattice in both the low-temperature, tetragonal phase, and the high-temperature cubic phase.

The magnitude of the ionic conductivity is expected to be proportional to the product of the concentrations of the mobile ions and the number of vacant sites, i.e., $c(1-c)$. For a disordered material with c around 0.5, small variations in the sodium concentration might not be expected to produce much change in the conductivity as neither the $c(1-c)$ term nor the number of carriers will change sharply. For both an increase in the sodium concentration (by admixture with Na_4SiO_4) and a decrease (by doping with Na_2SO_4), cubic phases stable, or metastable, at room temperature were obtained at low-dopant levels. In the latter case, the conductivities observed were indeed very close to those measured for the pure compound, although the silicate doping produced a sharp decrease in conductivity (Fig. 6).

The behavior of doping with $AlPO_4$ is perhaps the most interesting. There is an initial sharp drop in the conductivity at 300°C up to $x = 0.025$ (Fig. 2), but then an equally rapid rise to $x = 0.05$. For higher dopant levels the rate of increase slows, and there is a second maximum at $x = 0.2$. From $x = 0.3$ to 0.6 the conductivity decrease seems roughly linear with x and does not appear to show any obvious discontinuity through the change from crystalline to noncrystalline structures. For the

glassy phase at $x = 0.6$ the conductivity at 300°C (2×10^{-6} Ω^{-1} cm^{-1}) is roughly 3 orders of magnitude less than that of Na_3PO_4; it is, however, one of the highest measured for noncrystalline phases.

The high sodium-ion mobility in the glassy phase indicates that several features of the crystalline structure are retained, including positional disorder. The lack of any sharp change in conductivity as the structure changes from crystalline to noncrystalline indicates quite strongly the possibility of two-phase behavior in the apparently crystalline high-dopant compounds and could well account for the continuous decrease in resistivity from $x = 0.2$ through the crystal-glass transition composition. The rather sharp conductivity minimum at $x = 0.025$ could well have a crystallographic origin, however, with aluminum initially occupying a blocking site ($0 < x < 0.025$) and then a relatively non-blocking one so that the conductivity rises as the concentration of vacancies increases ($0.025 < x < 0.2$). This isothermal variation of the conductivity with aluminum content is not an artifact of the particular temperature chosen (300°C). From Fig. 2 it is seen that a similar effect would be observed, for example, at 350°C when all the compositions will be well within the high-temperature phase region. At the lowest dopant concentrations ($x = 0.01$ and 0.025), where the tetragonal-to-cubic phase transition is still observable crystallographically, the effect of this is also clearly revealed in the conductivity plots, in contrast to the situation for the undoped compound. The hysteresis observed for these compositions indicates the sluggishness of the phase transition in doped Na_3PO_4 and it was not manifested, either crystallographically or in the conductivity data, for $x > 0.05$.

It is interesting to compare the activation energies (E_A) that have been observed for ionic motion in the high conductivity phases of A_xBO_4 type compounds where A is lithium or sodium and BO_4 is sulfate, tungstate, or phosphate. $E_A \sim 0.4$ eV for lithium sulfate (*6*) and tungstate (*18*). Lithium phosphate has $E_A \sim 1.3$ eV (*19*); this compound has a conductivity of only $\sim 10^{-9}$ Ω^{-1} cm^{-1} at 300°C and does not show a discontinuous increase to a high-conductivity phase. However, on doping with 60 mole% Li_4SiO_4, a fast ion conducting composition is obtained with $\sigma \simeq 2 \times 10^{-2}$ Ω^{-1} cm^{-1} at 300°C and $E_A \sim 0.5$ eV (*19*). The analogous sodium compounds, on the other hand, have much higher activation energies ($Na_2WO_4 \sim 1.1$ eV (*20*) and $Na_3PO_4 \sim 0.8$ eV); but they do exhibit relatively high conductivity. The apparently characteristic difference in activation energy between the lithium and sodium compounds is presumably related to differences in the mechanism of conduction reflecting, particularly, ionic size effects. There is a possible connection of this behavior to the possible rotation of the anion groups in some of these phases (*5*) although neither the structural basis of these differences, nor of the other differences observed between sodium and lithium conductivities (in β-alumina for example), are presently well established. High-temperature diffraction experiments on some simple oxyanion conductors are in progress, which it is hoped may provide a background for suggesting possible useful compositions for further study, and indeed, the diffraction pattern of high-temperature lithium sulfate (*21*) shows much more markedly than high-temperature sodium phosphate (*15*) the manifestations of the structural disorder exhibited by fast ion conductors. It seems unlikely at the moment, that sodium compounds of this type will exhibit very high conductivities at moderate temperatures unless the activation energy can be reduced by some means.

In summary, we have shown that fast sodium ion conduction can be found in simple compounds at 300°C and below and a glassy phase at high-dopant levels of $AlPO_4$ in Na_3PO_4 was discovered which also shows high ionic conductivity. Only tentative interpretations of the observed behavior could be given; but the high activation energies for ionic

conduction seem to be characteristic of sodium compounds of this type.

Acknowledgment

Helpful discussions with A. E. Hughes are gratefully acknowledged.

References

1. N. Weber and J. T. Kummer, Adv. Energy Conv. Eng., ASME Conf., Florida, p. 913 (1967); J. R. Birk, *in* "Superionic Conductors" (G. D. Mahan and W. L. Roth, Eds.), p. 1, Plenum, New York/London (1976).
2. P. McGeehin and A. Hooper, *J. Mater. Sci.* **12**, 1 (1977).
3. See for example, A. Hooper, *J. Phys. D* **10**, 1487 (1977); J. E. Bauerle, *J. Phys. Chem. Solids* **30**, 2657 (1969).
4. M. Palazzi and F. Remy, *Bull. Soc. Chim. Fr.* **8**, 2795 (1971).
5. T. Forland and J. Krogh-Moe, *Acta Chem. Scand.* **11**, 565 (1957).
6. A. Kvist and A. Lunden, *Z. Naturforsch. A* **20**, 235 (1965).
7. T. Takahashi, S. Ikeda, and O. Yamamoto, *J. Electrochem. Soc.* **119**, 477 (1972).
8. J. B. Goodenough, H. Y. P. Hong, and J. A. Kafalas, *Mater. Res. Bull.* **11**, 203 (1976).
9. B. E. Liebert and R. A. Huggins, *Mater. Res. Bull.* **11**, 533 (1976).
10. I. D. Raistrick, C. Ho, and R. A. Huggins, *J. Electrochem. Soc.* **123**, 1469 (1976).
11. I. M. Hodge, M. D. Ingram, and A. R. West, *J. Amer. Ceram. Soc.* **59**, 360 (1976).
12. P. H. Bottelberghs and W. Van Gool (Eds.) "Fast ion Transport in Solids," p. 637, North-Holland, Amsterdam (1973).
13. G. C. Farrington and W. L. Roth, *Electrochim. Acta* **22**, 767 (1977).
14. A. Bengtzelius, A. Kvist, and A. Lunden, *J. Phys.* **34**, C9–119 (1973); A. Kvist, A. Bengtzelius, and U. Trolle, *Z. Naturforsch.* **239**, 2042 (1968).
15. J. M. Newsam and B. C. Tofield, unpublished data.
16. L. Helmholz, *J. Chem. Phys.* **4**, 316 (1936).
17. O. V. Mazurin, Electrical Properties and Structure of Glass, Consultants Bureau, New York (1965).
18. A. Kvist and A. Lunden, *Z. Naturforsch. A* **21**, 1509 (1966).
19. Y. W. Hu, I. D. Raistrick, and R. A. Huggins, *Mater. Res. Bull.* **11**, 1227 (1976).
20. P. H. Bottelberghs and F. R. Van Buren, *J. Solid State Chem.* **13**, 182 (1975).
21. L. Nilsson, J. O. Thomas, and B. C. Tofield, unpublished data.